Journal of Materials Chemistry C

ROYAL SOCIETY OF CHEMISTRY

PAPER

View Article Online
View Journal | View Issue

Cite this: J. Mater. Chem. C, 2023, 11, 2949

Activity of N–H in phenothiazine derivatives: synthesis and applications in fluoride ions sensing and electrochromism†

Weidong Zhang,*[a] Xiucun Feng,[a] Chao Zhang,[a] Qiangqiang Jia,[d] Xingliang Liu*[a] and Kun Zhou*[bc]

Received 27th September 2022,
Accepted 25th January 2023

DOI: 10.1039/d2tc04079d

rsc.li/materials-c

A series of phenothiazine derivatives containing N–H, **3a**, **3b**, **3c** and a N-substituted phenothiazine derivative, **3d** were synthesized. These phenothiazine derivatives exhibited good air/moisture stability and excellent fluorescence properties. They showed excellent chromic behaviour in response to multiple external stimuli, especially fluoride ions and the application of electric voltages. The addition of fluoride ions to these phenothiazine derivatives induced a rapid change in the emission colour from blue to yellow, accompanied by significant changes in the emission intensity. This response was shown to be highly selective to fluoride ions. Films deposited from solutions of a blend of **3a** and polycaprolactone also demonstrated a good ratiometric sensing ability for fluoride ions. Electrochromic devices (ECDs) fabricated from these composites exhibited reversible changes in color that depended on the applied voltage.

1. Introduction

Driven by the increasing importance of intelligent technology, significant progress has been made in recent times in the development of stimuli-sensitive, ''intelligent'' materials for various applications, which include mimicking photosynthesis,[1–3] catalysis,[4] diverse biological applications,[5–7] sensing,[8–11] and smart windows.[12,13] As highly reactive intermediate species, organic radicals play an important role in the fabrication and the characteristic properties of numerous engineered, stimuli sensitive-materials. Recently, chemists and materials scientists have given a lot of attention to long-lived, organic radical species that have unique electronic properties due to their magnetic spin moments arising from singly occupied molecular orbitals.[14–16] However, they come with their own set of challenges because these radicals generally tend to be very reactive, and unstable, as well as mono-stimuli-responsive. Thus, the development of novel, long-lived, and fast, multi-stimuli-responsive radical species is vital to the development of applications that can exploit their unique properties.

The phenothiazine (PTZ) unit is an electron-rich tricyclic heteroarene, characterized by the presence of powerful electron donors like nitrogen and sulphur atoms. PTZ materials typically exhibit relatively intense luminescence, high photoconductivity, and reversible oxidation.[17–19] The success of PTZ-based optoelectronic devices is attributed to the stable, heterocyclic structure of their radical cations. A region of significant electron density, primarily localized on the sulphur atom in the phenothiazine core scaffold, is associated with electrophores, producing dyads and triads. This makes the phenothiazine unit highly sensitive to oxidizing agents and is especially susceptible to electronic substitutions at the 3, or 7-position. PTZ has tuneable redox properties and can exhibit reversible and fast electron transfer reactions to form stable neutral, monocation, and dication radicals.[20–22] Because of the presence of electron-rich sulphur and nitrogen heteroatoms, and an ionization potential of 6.73 eV, phenothiazine is well suited for the synthesis of donor–acceptor (D–A) materials with enhanced intramolecular charge transfer (ICT) characteristics in the ground state and photoinduced electron transfer (PET) properties in the excited-state, which are widely used as photoactive materials in organic electronic devices, such as organic light-emitting diodes (OLEDs), organic field effect transistors

[a] School of Chemical Engineering, Qinghai University, Xining, 810016, China. E-mail: zhangwd@qhu.edu.cn
[b] School of Science and Engineering, Shenzhen Institute of Aggregate Science and Technology, The Chinese University of Hong Kong, Shenzhen, Guangdong 518172, China. E-mail: zhoukun@cuhk.edu.cn
[c] Guangdong Provincial Key Laboratory of Luminescence from Molecular Aggregates (South China University of Technology), Guangzhou 510640, China
[d] State Key Laboratory of Plateau Ecology and Agriculture, Qinghai University, Xining, 810016, China

† Electronic supplementary information (ESI) available: Experimental details, NMR spectra for all the new compounds, cyclic voltammogram data and results of theoretical calculations. See DOI: https://doi.org/10.1039/d2tc04079d

(OFETs), chemical sensors, organic solar cells (OSCs), and batteries.[23–27] However, most these photoactive materials use the protected PTZ structure (N-substituted phenothiazine derivatives), in which the nitrogen atom at the 10-position (10 N–H) is replaced by a covalent group.[28–30]

Because of its highest charge density and Lewis basic nature, fluoride has received well-deserved attention from the scientific community owing to its association with a diverse array of biological, medical, and technological processes.[31–33] Since the fluoride ion is a strong hydrogen bond acceptor, a large number of optical sensors have been developed based on fluoride induced deprotonation through H-bonding for detecting fluoride ions. However, most of the H-bonding type fluoride ion sensors involve expensive and lengthy synthetic protocols and show relatively poor selectivity, especially interfered by alkaline anions like AcO^- and $H_2PO_4^-$.[34,35] Therefore, the development of simple organic receptors containing functional groups or heterocyclic rings proficient for the selective detection of fluoride with high selectivity and sensitivity have become a highly popular topic of interest to scientists. PTZ materials are typical excited-state intramolecular proton transfer (ESIPT) materials,[36] in which the acidity of the H-bond donor within the ICT chromophores can be synthetically manipulated to allow selective interaction with the basic fluoride. Based on these considerations, we synthesized the phenothiazine derivatives by a typical Suzuki–Miyaura coupling reaction, which were successfully used as chemosensors for the ratiometric detection of F^- with high selectivity and sensitivity.

Electrochromism is a phenomenon in which the colour of a material changes reversibly depending on the redox reactions when an electrical potential is applied. This feature is very important for a wide range of applications such as smart windows, screens, solar-to-fuel conversion, sensors, energy storage, and versatile functional electrochromic displays.[37,38] In recent years, a lot of research has focused on electrochromic materials like transition metal oxides, organic molecules (viologens), and polymeric electrochromic materials, which can achieve electro-induced colouration and colour switching on the application of an external voltage.[39–44] Whereas, because of the complex synthesis process and unstable radical cation, those materials would be the limiting factor for excellent device performance and broader applications. Therefore, we successfully used the phenothiazine derivatives in devices on account of the highly stable radical cation, and they showed excellent advantages as electrochromic materials.

2. Results and discussion

2.1 Synthesis and characterization

Precursor **2** was synthesized as described by Xiao-Qing Zhu, *et al.*[45] 10*H*-Phenothiazine was suspended in glacial acetic acid and a solution of bromine in glacial acetic acid was added dropwise with continuous stirring to yield compound **2** as green crystals. A typical Suzuki-Miyaura coupling reaction, significantly modified to avoid column chromatography, was carried out. Precursor **2** was dissolved in a boiling, 10 : 1 mixture of ethoxyethanol and water under a nitrogen atmosphere. Immediately after that, aromatic boronic acid, potassium carbonate, and $Pd(PPh_3)_4$ were added with vigorous stirring at 130 °C for 30 minutes to get the compounds **3a**, **3b**, and **3c**, with yields of 93%, 95%, and 92%, respectively. The peak of N–H in the phenothiazine unit appears at 8.906 ppm (**3a**), 8.847 ppm (**3b**), and 9.084 ppm (**3c**). The N-substituted phenothiazine derivative **3d** was also successfully synthesized with an 86% yield (Scheme 1). The intermediate and the target molecules were characterized by ^1H and ^{13}C nuclear magnetic resonance (NMR) spectroscopy, high-resolution mass spectrometry (HRMS) and elemental analyses (C, H and N).

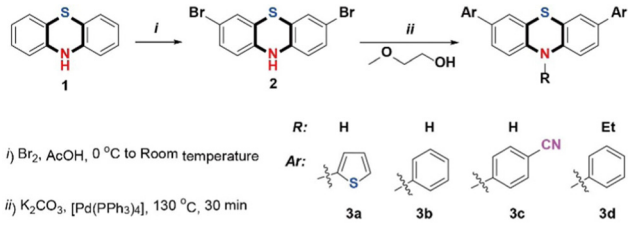

Scheme 1 Synthetic procedures for **3a**, **3b**, **3c** and **3d**.

2.2. Photophysical properties

Phenothiazine derivatives are well-known as fluorophores and are widely used as conjugated components in luminescent organic materials.[46] As compared to the photophysical and electrochemical properties of the N-substituted phenothiazine derivative **3d**, the derivatives **3a**, **3b**, and **3c** provided a clear-cut view of the characteristic properties. It was found that the absorption maxima of **3a**, **3b**, and **3c** increased gradually, while their band gaps decreased. The phenothiazine derivative **3a**, modified with thienyl moieties, showed the lowest-energy absorption peak and the major absorption band at 296 nm was assigned to the π–π* transitions of the aromatic rings and the absorption peaks at 363 nm was attributed to the stronger electron-donating character of the thiophene unit,[47] while it showed maximum emission at 476 nm (Φ = 0.18, τ = 1.43 ns) (Fig. 1 and Table 1 and Fig. S2–S6, S12, ESI†). A similar phenomenon was also observed for **3b** (λ_{max} = 338 nm, $\lambda_{max,em}$ = 461 nm, Φ = 0.46, τ = 4.39 ns), which means extended directions of electron-donating moieties can affect the electron transfer

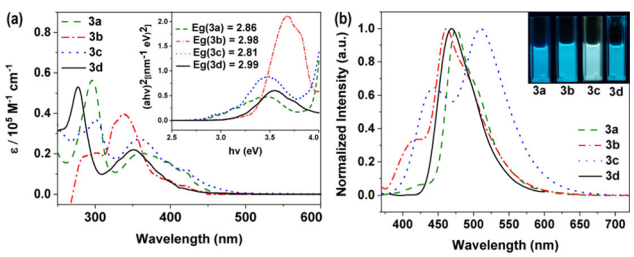

Fig. 1 UV-Vis absorption spectra (left) and photoluminescence (PL) spectra (right) of the phenothiazine derivatives in THF solutions; the extrapolated optical band gaps (E_g) is shown as insets.

Table 1 Photophysical data for the phenothiazine derivatives

Comp.	λ_{abs}[a] (nm)	ε (10^5 M^{-1} cm^{-1})	λ_{em}[b] (nm)	SS[c] (cm^{-1})	τ[d] (ns)	QY[e] (%)
3a	363	0.27	476	6539	1.43	18
3b	338	0.40	461	7894	4.39	46
3c	360	0.20	510	8170	4.38	40
3d	351	0.22	466	7031	5.64	37

[a] The longest λ_{max} values in the UV-Vis spectra. [b] Emission maxima in THF. [c] Stokes shift = $1/\lambda_{abs} - 1/\lambda_{em}$. [d] Lifetimes in THF. [e] Quantum yield in THF.

process.[48] Due to the growth of conjugated chains and the introduction of the electrophilic –CN units into the structures, the absorption spectrum of **3c** showed maxima at 301 nm and 360 nm, and the emission spectra showed a local maximum at 510 nm (Φ = 0.40, τ = 4.38 ns), which indicated a slight bathochromic shift caused by electron transfer from the phenothiazine donor to the –CN acceptor compared to **3a** and **3b**.

2.3 Redox properties

The electrochemical characteristics of the phenothiazine derivatives were studied by cyclic voltammetry (CV) in DMF solution (Fig. S7, ESI†). The results are summarized in Table S5, ESI.† These CV curves show that all the phenothiazine derivatives have a reversible one-electron reductions process, and the redox potentials of **3a**, **3b**, **3c** and **3d** were measured to be −1.15 (E_{LUMO} = −3.65 eV), −1.08 (E_{LUMO} = −3.72 eV), −1.16 (E_{LUMO} = −3.64 eV), and −1.20 V (E_{LUMO} = −3.60 eV) (*vs.* Fc/Fc^+), respectively (Fig. 2 and Fig. S8–S11, ESI†). Therefore, substitution with moieties with different electron-donating abilities has very little effect on the reduction potential of the phenothiazine derivatives and the relatively low LUMO (lowest unoccupied molecular orbital) energy levels.[28,49] However, mutual orthogonalization of the substituent groups indicates that the electrophilic –CN group is effective and even causes a shift of the anodic reduction potential of **3c**. The highest occupied molecular orbital (HOMO) levels, as calculated from the LUMO levels and the optical band gaps (**3a**, 2.86 eV; **3b**, 2.98 eV; **3c**, 2.81 eV; **3d**, 2.99 eV), were −6.51, −6.70, −6.45 and −6.59 eV, respectively, mimic the trend shown by the calculated values.

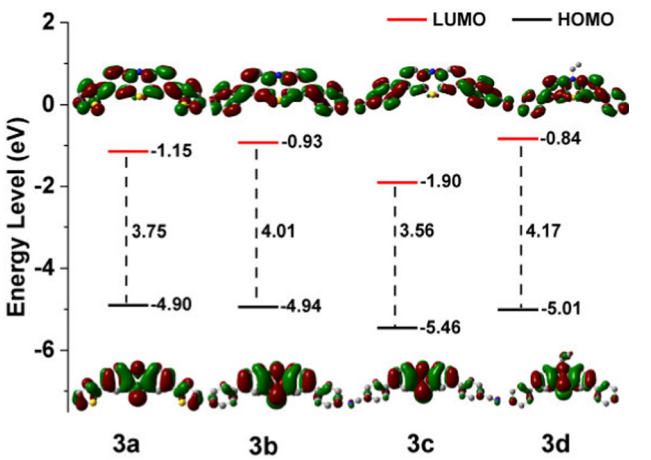

Fig. 2 Experimental orbital energy levels and HOMO/LUMO orbital plots of **3a**, **3b**, **3c** and **3d**.

2.4. Ratiometric fluoride-ion sensing properties

The combination of an anion acceptor with a chromogenic moiety is a convenient and efficient strategy for designing a colourimetric anion sensor, in which the targeted binding event is manifested as a colour change visible to the naked eye.[50] Many specific photophysical behaviors of these compounds for binding F^- ions were developed.[35,51–53] Considering the existence of the N–H bond in the phenothiazine derivatives, we decided to investigate the response of these compounds to fluoride anions using UV-vis and fluorescence titration experiments, which were carried out using a solution of *n*-tetrabutylammonium fluoride (TBAF), which was added to the prepared solutions (10 μM) with a certain number of compounds every time. As shown in Fig. 3a, the titration of **3a** with TBAF (1 mM in THF) resulted in a gradual decrease in the maximum absorption intensity at 297 nm, accompanied by the formation of a new absorption

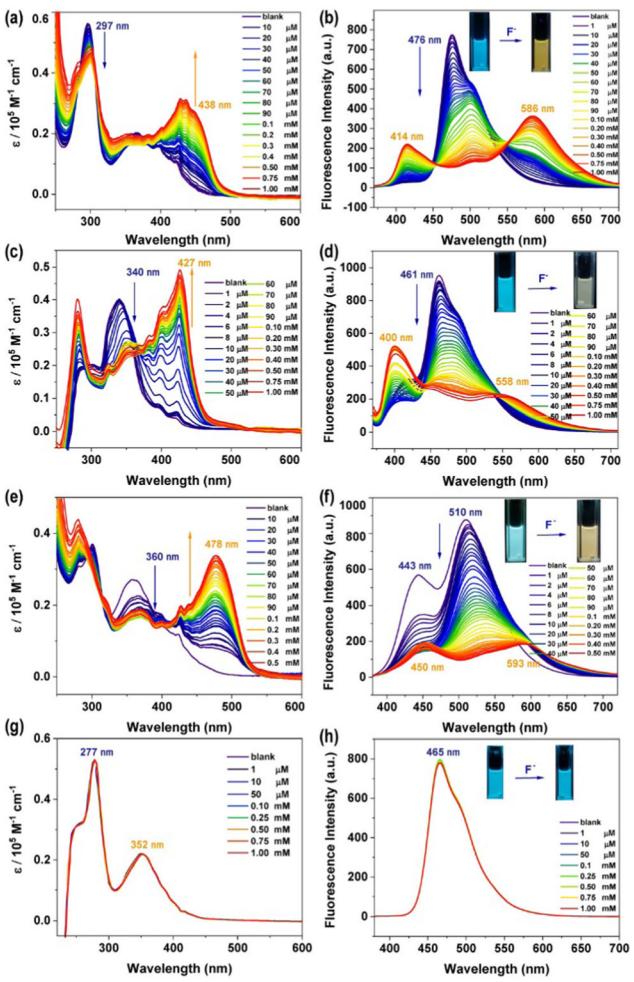

Fig. 3 Spectral changes in the UV/vis absorption (left) and fluorescence (right) after the addition of TBAF. (a) and (b) **3a**, λ_{ex} = 365 nm, [**3a**] = 10 μM; (c) and (d) **3b**, λ_{ex} = 365 nm, [**3b**] = 10 μM; **3c**, λ_{ex} = 365 nm, [**3c**] = 10 μM; **3d**, λ_{ex} = 365 nm, [**3d**] = 10 μM.

peak at 438 nm. In addition, upon excitation at 365 nm, the addition of F^- ions cause a drastic decrease in emission at 476 nm and the simultaneous appearance of two new emission bands at 414 nm and 586 nm (Fig. 3b), which is manifested in the emission colour changing from blue to deep yellow after titration. This may be due to the PTZ derivative **3a** undergoing hydrogen bond formation and the subsequent deprotonation of the N–H.[54,55] Compounds **3b** and **3c** also exhibited almost identical titration behaviour (Fig. 3c–f). The UV-vis spectra of **3b** (λ_{max} = 340 nm) and **3c** (λ_{max} = 360 nm) showed a gradual decrease in the absorption intensity at 340 nm and 360 nm respectively and the emergence of a new absorption peak in each spectrum at 427 nm and 478 nm, which further intensified on binding of F^-. A similar phenomenon was observed in the fluorescence spectra, where the emissions of **3b** (λ_{em} = 461 nm) and **3c** (λ_{em} = 510 nm) gradually decreased with the addition of F^-, and two new emission bands appeared in each spectrum (**3b:** λ_{em} = 400 and 558 nm, **3c:** λ_{em} = 450 and 593 nm) that steadily grew with the addition of more F^- solution due to mono-deprotonation processes.[56] The behavior of the N-substituted phenothiazine derivative **3d**, as characterized by UV-vis and fluorescence titration experiments, was significantly different from that of **3a**, **3b**, and **3c** after the addition of fluoride ions (Fig. 3g and f). The absorption and emission bands of **3d** showed almost no change even at a F^- concentration of 1 mM. This remarkable difference between the phenothiazine derivatives and the N-substituted phenothiazine derivative implies the existence of a strong ground state F···H–N interaction for the PTZ derivatives **3a**, **3b**, and **3c**, which was confirmed through DFT calculations (Fig. S13, ESI†). To better understand the origin of the observed response of N–H to fluoride ions, corresponding experiments were performed on **3a** as a molecular model system. Upon addition of different equivalents of TBAF to compound **3a**, the N–H signal in the phenothiazine unit that appeared at 8.906 ppm gradually decreased, indicating the formation of a **3a–F** complex (Fig. S14, ESI†). These results also mean that an instantaneous colour change from blue to yellow occurs, an event that allows visible, naked eye detection of fluoride. The as-calculated detection limits (DL), based on three times the standard deviation regulation,[57] were 31.7 μM, 41.6 μM, and 48.5 μM, respectively (Fig. S15–S19, ESI†).

The anion sensing properties of the selectivity of the phenothiazine derivatives were assessed by the simultaneous addition of a certain amount of different anions such as F^-, Cl^-, Br^-, I^-, NO_3^-, ClO_4^-, BF_4^-, PF_6^-, AcO^-, $H_2PO_4^-$, and SO_4^{2-}. Histograms of (I_0/I)-1 plotted against concentrations of F^- and other anions (Fig. 4 and Fig. S21, S22, ESI†) showed that the fluorescence spectra of **3a** showed distinct changes both in intensity and emission wavelength upon the addition of fluoride anions, while other anions did not have any significant effect, except for some slight interference due to AcO^-. Similarly, due to the differences in the basicity and the ability of the aforementioned anions to form hydrogen bonds, **3b** and **3c** showed a highly selective response to the fluoride anions (apart from a marginal response to AcO^- anions). This anion-specific behaviour shows

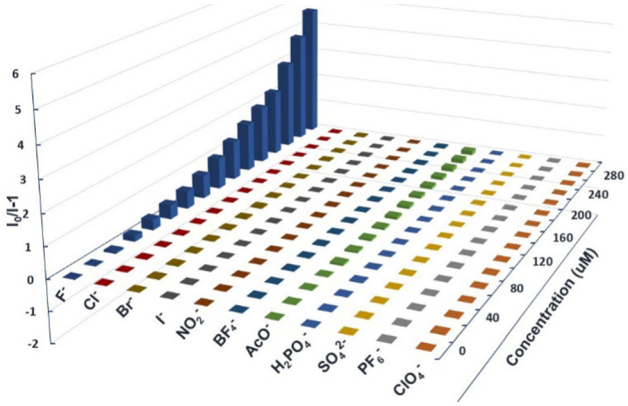

Fig. 4 (I_0/I)-1 of 11 anions for the emission of **3a** in THF (10 μM in THF) at different equivalents of anions.

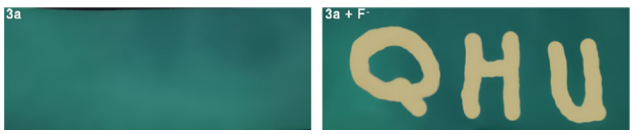

Fig. 5 The **3a** based film sensors for fluoride anions under UV irradiation (λ_{ex} = 365 nm).

that the phenothiazine derivatives **3a**, **3b**, and **3c** can be used as highly selective colourimetric sensors for the detection of fluoride.

A fluoride-sensing film (Fig. 5) was fabricated from a solution of **3a** and polycaprolactone (PCL) (weight ratio: 1/400) in THF. While this film showed blue-green luminescence visible to the naked eye under ultraviolet irradiation (λ_{ex} = 365 nm), on exposure to a fluoride solution, a yellow luminescence was observed and the detection limit was 0.1 mM (Fig. S20, ESI†). This demonstrated the excellent potential of **3a** for optoelectronic applications as solid-state fluoride ion sensors.

2.5 Fabrication of electrochromic devices (ECDs) and spectroelectrochemical properties

Some proof-of-concept electrochromic devices were fabricated to explore the application of these phenothiazine derivatives. To facilitate the observation of the colour changes and electrochromic behaviour of these new electrochromic composites, fluorine-doped tin oxide (ITO)-coated glasses,[58–60] because of the good light transmission and electrical conductivity, were used as electrodes, and **3a**/**3b**/**3c**/**3d** were used as the active components. Fig. 6 shows the observed colour changes and the spectroelectrochemical data of the devices based on these phenothiazine derivatives in DMF solution at different voltages. A direct current instrument was attached to this electrochromic device, and when the voltage was set between 0 V and −3.5 V, as shown in Fig. 6b, a yellow colouration was observed in the neutral state, with the UV-vis absorption maxima below 400 nm without an applied potential. On gradually increasing the potential from 0 V to −1.5 V, a colour change from yellow to green could be observed, with an increase in the intensities of

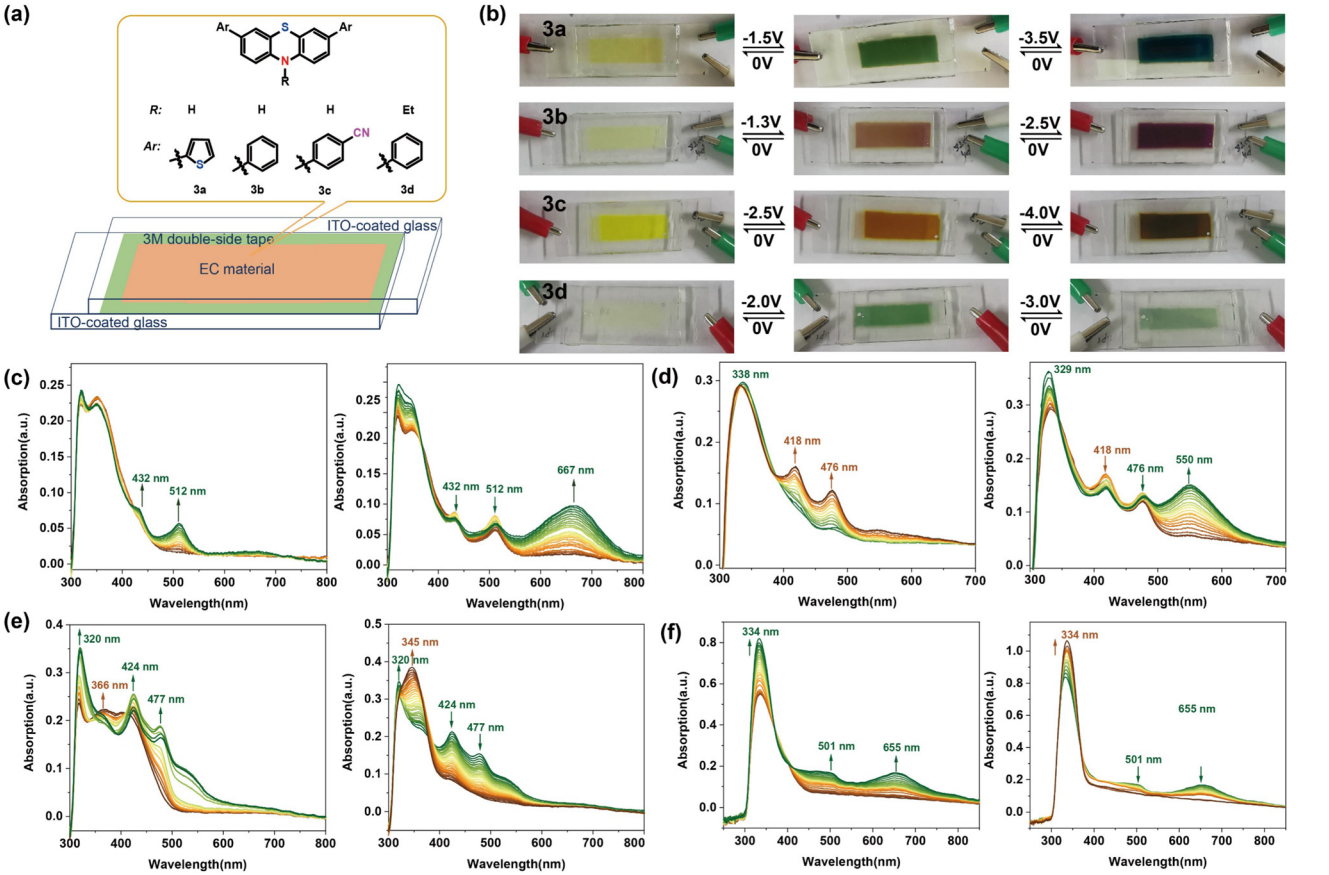

Fig. 6 (a) Schematic of the proof-of-concept electrochromic device; (b) photos of the ECDs under different voltages; (c) spectroelectrochemistry of **3a** in DMF solution (potential: 0 to −3.5 V); (d) spectroelectrochemistry of **3b** in DMF solution (potential: 0 to −2.5 V); (e) spectroelectrochemistry of **3c** in DMF solution (potential: 0 to −4.0 V); (f) spectroelectrochemistry of **3d** in DMF solution (potential: 0 to −3.0 V).

the absorption bands at 432 and 512 nm. The new species are thought to be the radical cations produced in the electrochemical oxidation process.[61] A deep teal color was observed and the UV-vis absorption peak at 667 nm further intensified as the potential was changed from −1.5 to −3.5 V. A further decrease in the UV-vis absorption intensity was seen with a further increase in the potential over −3.5 V (Fig. 6c). The ECD containing **3b** appears light yellow (its original colour) at 0 V. When the applied voltage is changed from 0 to −1.3 V, the absorption intensities around the wavelength bands of 418 nm and 476 nm increased due to the formation of the new radical species, and the device colour changed to brown. Moreover, when the potential was further changed from −1.3 to −2.5 V, the absorption intensity for wavelengths around 550 nm increased to some extent, and the colour of the ECD changed to dark brown (Fig. 6d). We observed that whenever the application of the voltage was stopped, the colour recovered to the original light yellow accompanied by absorption intensities at 418 nm, 476 nm and 550 nm decreasing to those seen originally. This demonstrated good, reversible electrochromic switching capability (Fig. S24, ESI†). The changes in colour and absorption intensity of **3c** in the visible range of wavelengths were similar (Fig. 6e). This shows that the phenothiazine derivatives could function as electrochromic devices switching between two colours. The original ECD containing **3d**, which was nearly colourless at 0 V, turned green when the applied voltage was changed to −2.0 V with an increase in the absorption intensity around the wavelengths of 501 nm and 655 nm. However, on further increasing the potential to −3 V, the intensity of the green colour decreased (due to a decrease in absorption intensity). The proposed mechanism for the electrochromism of **3a** can be described in Fig. S23 (ESI†). The colour changes of **3a** can be attributed to the different oxidation states, which were confirmed through DFT calculations. Moreover, the ECDs fabricated from **3a**, **3b**, and **3c** continued to show reversible colour changes even after 30 cycles, while, the performance of the ECD of **3d** declined significantly after several cycles (Fig. S24, ESI†).

3. Conclusions

In summary, a novel phenothiazine derivative material with N–H has been synthesized and characterized. The results showed that the PTZ derivatives **3a**, **3b**, and **3c** showed good stability and bright, intense fluorescence, which made them suitable for the colourimetric detection of fluoride ions among the common interferents, manifesting as a change in the

fluorescence intensity and colour (from blue to yellow). In contrast, the N-substituted phenothiazine derivative (**3d**) did not show any conspicuous change in fluorescent emissions even after increasing the F^- concentration to 1 mM, which implied the existence of a strong ground state F···H–N interaction for **3a**, **3b**, and **3c**. With multiple redox centers and light absorption in the visible region, the proof-of-concept of solution-based ECDs were demonstrated successfully. The integration of two kinds of applications of the phenothiazine derivative would provide an effective strategy for developing applications of multi-stimuli-responsive materials. We are continuing further research and development on the detection of fluoride anions in aqueous media, enhancing their electrochromic performance, and increasing their potential applications.

4. Experimental

General

All commercially available chemicals were used without further purification unless otherwise noted. THF was distilled from sodium/benzophenone prior to use. Ethoxyethanol, tetrakis-(triphenylphosphine) palladium ($Pd(Ph_3P)_4$) (99%), potassium carbonate (99%), thiophene-2-boronic acid (99%), phenylboronic acid (99%), 4-cyanophenyl)boronic acid (99%) and bromoethane (99%) were purchased from Energy Chemical Inc. 3,7-Dibromo-10*H*-phenothiazine (**2**) was prepared according to the literature procedures.[62]

NMR spectra were measured on a Bruker Avance-600 spectrometer in the solvents indicated; chemical shifts are reported in units (ppm) by assigning the TMS resonance in the ^{1}H spectrum as 7.26 ppm, and the $CDCl_3$ resonance in the ^{13}C spectrum as 77.0 ppm. Coupling constants are reported in Hz with multiplicities denoted as s (singlet), d (doublet), t (triplet), q (quartet) and m (multiplet). UV-vis measurements were performed using a DH-2000-BAL scan spectrophotometer. Fluorescence measurements were conducted on a FLS920 system. The cyclic voltammetry (CV) spectra were measured using a Metrohm PGSTAT204 set up.

All the computational calculations reported in this work were performed using the Gaussian 09 code. The geometries for the ground state of these compounds were optimized at the B3LYP[3,4]-D3 hybrid functional, and the 6-311G(d,p) basis set for **3a**, **3b**, **3c**, and **3d**, and the 6-311+G(d,p) basis set for **3a–F**.

Synthetic procedures

General procedure for the synthesis of 3a–c. 3,7-Dibromo-10*H*-phenothiazine (**2**) (3.57 g, 10.0 mmol) was dissolved in a boiling mixture of ethoxyethanol and water (10 : 1, 110 mL). To the resulting green solution, a finely ground mixture of arylboronic acid (28.0 mmol, 2.80 equiv.), K_2CO_3 (7.73 g, 56.0 mmol, 5.60 equiv.) and $Pd(PPh_3)_4$ (200 mg, 0.17 mmol, 1.73 mol%) was added immediately under vigorous stirring. The reaction mixture was kept under reflux conditions at 130 °C for 30 minutes and then was allowed to cool to room temperature. The product precipitated during cooling. The suspension was diluted with deionized water (100 mL) to increase precipitation. The crude product was filtered over a Büchner funnel, washed with ethanol and cold acetone (3 × 30 mL each) and air dried to give compounds **3a–c**.

3,7-Di(thiophen-2-yl)-10*H*-phenothiazine (3a). Yellow crystals. Yield of 93%. ^{1}H NMR (600 MHz, DMSO): δ 8.91(s, 1H, N–H), 7.44 (d, 2H, J = 4.8 Hz, Ar*H*), 7.36 (d, 2H, J = 3.6 Hz, Ar*H*), 7.27 (d, 2H, J = 8.4 Hz, Ar*H*), 7.23 (s, 2H, Ar*H*), 7.08 (t, 2H, J = 4.2 Hz, Ar*H*), 6.69 (d, 2H, J = 8.4 Hz, Ar*H*); 13C NMR (151 MHz, DMSO): δ 143.1, 141.1, 128.8, 128.3, 125.5, 124.9, 123.4, 122.9, 117.2, 115.3. HRMS (APCI) *m/z*: $[M + H]^+$ calcd for $C_{20}H_{13}NS_3$, 364.0288, found, 364.0265. Anal. calcd For $C_{20}H_{13}NS_3$: C, 66.08; H, 3.60; N, 3.85. Found: C, 66.12; H, 3.71; N, 3.92. Fluorescence emission (in THF) (λ_{ex} = 365 nm): λ_{emis} = 476 nm (quantum yield Φ = 0.18; lifetime, τ = 1.43 ns).

3,7-Diphenyl-10*H*-phenothiazine (3b). Yellow crystals. Yield of 95%. ^{1}H NMR (600 MHz, DMSO): δ 8.85(s, 1H, N–H), 7.58 (d, 2H, J = 7.2 Hz, Ar*H*), 7.42–7.40 (m, 4H, Ar*H*), 7.33–7.28 (m, 4H, Ar*H*), 7.25 (d, 2H, J = 1.8Hz, Ar*H*), 6.77 (d, 2H, J = 8.4 Hz, Ar*H*); ^{13}C NMR (151 MHz, DMSO): δ 141.4, 139.6, 134.3, 129.3, 127.3, 126.4, 126.2, 124.6, 117.3, 115.3. HRMS (APCI) *m/z*: $[M + H]^+$ calcd for $C_{24}H_{17}NS$, 352.1160, found, 352.1142. Anal. calcd For $C_{24}H_{17}NS$: C, 82.02; H, 4.88; N, 3.99. Found: C, 82.14; H, 4.93; N, 4.06. Fluorescence emission (in THF) (λ_{ex} = 365 nm): λ_{emis} = 461 nm (quantum yields Φ = 0.46; lifetime, τ = 4.39 ns).

4,4′-(10*H*-Phenothiazine-3,7-diyl)dibenzonitrile (3c). Brown crystals. Yield of 92%. ^{1}H NMR (600 MHz, DMSO): δ 9.08(s, 1H, N–H), 7.83 (dd, 8H, J = 24 Hz, 8.4 Hz, Ar*H*), 7.43 (dd, 2H, J = 8.4 Hz, 1.2 Hz, Ar*H*), 7.38(s, 2H, Ar*H*), 6.77(d, 2H, J = 8.4 Hz, ArH); ^{13}C NMR (151 MHz, DMSO): δ 143.9, 142.0, 133.2, 132.2, 127.0, 126.8, 125.1, 119.5, 117.5, 115.4, 109.6. HRMS (APCI) *m/z*: $[M + H]^+$ calcd for $C_{26}H_{15}N_3S$, 402.1065, found, 402.1031. Anal. calcd For $C_{26}H_{15}N_3S$: C, 77.78; H, 3.77; N, 10.47. Found: C, 78.85; H, 3.87; N, 10.56. Fluorescence emission (in THF) (λ_{ex} = 365 nm): λ_{emis} = 510 nm (quantum yield Φ = 0.40; lifetime, τ = 4.38 ns).

10-Ethyl-3,7-diphenyl-10*H*-phenothiazine (3d). Sodium hydride (1.305 g, 32.62 mmol) was added to a solution of **3b** (8.76 g, 25.01 mmol) in anhydrous DMF (60 mL) in an oven-dried 100 mL round-bottomed flask under nitrogen atmosphere, which was immersed in an oil bath at 30 °C. The oil bath was then heated to 50 °C for 1 h. A reflux condenser was attached, and bromoethane (2.44 mL, 3.55 g, 32.6 mmol) was added to the reaction mixture dropwise through the condenser. The reaction mixture was then stirred for 5 h. Ice was added, and the organic product was extracted with ethyl acetate (3 × 40 mL). The combined organic layers were dried over $MgSO_4$, filtered to remove solids, and the filtrate was concentrated by rotary evaporation. The crude product was purified by column chromatography with hexanes as the eluent to give **3d** as white crystals. Yield: 8.15 g (86%). ^{1}H NMR (600 MHz, $CDCl_3$): 7.54 (d, 4H, J = 7.2 Hz, 8.4 Hz, Ar*H*), 7.43–7.397.38 (m, 8H, Ar*H*), 7.31 (t, 2H, J = 7.2 Hz, Ar*H*); 6.96 (d, 2H, J = 8.4 Hz, Ar*H*), 3.40 (s, 2H, CH_2), 1.48 (t, 3H, J = 7.2 Hz, CH_3); ^{13}C NMR (151 MHz, $CDCl_3$): δ 143.9, 140.0, 135.5, 128.8, 127.0, 126.5, 126.0, 125.8, 124.3, 115.2, 42.0, 13.0. HRMS (APCI) m/z: $[M + H]^+$ calcd for $C_{26}H_{21}NS$, 380.1473, found, 380.1461. Anal.

calcd For $C_{26}H_{21}NS$: C, 82.28; H, 5.58; N, 3.69. Found: C, 82.31; H, 5.61; N, 3.71. Fluorescence emission (in THF) (λ_{ex} = 365 nm): λ_{emis} = 465 nm (quantum yield Φ = 0.37; lifetime, τ = 5.64 ns).

Preparation of the film

Polycaprolactone (PCL) (4 g) was dissolved in 10 mL THF in a round bottom flask at 40 °C. After the solid was completely dissolved, compound **3a** (10 mg) was added dropwise at 40 °C, and was stirred for another 6 h. Then the solution above was further cast on a pre-cleaned glass substrate to fabricate the sensor films.

Fabrication of the electrochromic devices (ECDs)

The original ITO glasses were 100 × 100 × 1.1 mm and the resistance was 10 Ω. A glass cutter was used to cut the original ITO glasses for different types of ECDs. Two ITO-coated glasses (5 cm × 2 cm) were bent with 3 M double-side tapes (width: 4 mm, thickness: 0.5 mm) and a cavity formed between them. Compounds **3a–3d** were dissolved in DMF solution, $c \sim 5 \times 10^{-3}$ M, with ethyl-3-methylimidazolium bis(trifluoromethylsulfonyl) act as the supporting electrolyte. The solution was injected into the cavity by a syringe, then a UV-cured gasket was used to seal the cavity further.

Conflicts of interest

There are no conflicts to declare.

Acknowledgements

We gratefully acknowledge financial support from the Natural Science Foundation of China (Grants No. 22265027), the Project of Qinghai Science & Technology Department (Grant No. 2021-ZJ-979Q) and the Open Fund of Guangdong Provincial Key Laboratory of Luminescence from Molecular Aggregates (No. 2019B030301003), Guangzhou 510640, China (South China University of Technology).

Notes and references

1 T. Hisatomi, J. Kubota and K. Domen, *Chem. Soc. Rev.*, 2014, **43**, 7520–7535.
2 J. Hou, O. Inganas, R. H. Friend and F. Gao, *Nat. Mater.*, 2018, **17**, 119–128.
3 A. K. Jena, A. Kulkarni and T. Miyasaka, *Chem. Rev.*, 2019, **119**, 3036–3103.
4 S. Yuan, L. Feng, K. Wang, J. Pang, M. Bosch, C. Lollar, Y. Sun, J. Qin, X. Yang, P. Zhang, Q. Wang, L. Zou, Y. Zhang, L. Zhang, Y. Fang, J. Li and H.-C. Zhou, *Adv. Mater.*, 2018, **30**, 1704303.
5 C. He, X. Zhuang, Z. Tang, H. Tian and X. Chen, *Adv. Healthcare Mater.*, 2012, **1**, 48–78.
6 T. Urbanek, E. Jaeger, A. Jaeger and M. Hruby, *Polymers*, 2019, **11**, 1061–1082.
7 A. Beck, F. Obst, D. Gruner, A. Voigt, P. J. Mehner, S. Gruenzner, R. Koerbitz, M. H. Shahadha, A. Kutscher, G. Paschew, U. Marschner and A. Richter, *Adv. Mater. Technol.*, 2022, 2200417.
8 Y.-S. Lim, J. S. Kim, J. H. Choi, J. M. Kim and T. S. Shim, *Colloid Interface Sci. Commun.*, 2022, **48**, 100624.
9 B. Meng, Y. Zhang and P.-C. Ma, *Macromol. Chem. Phys.*, 2020, **221**, 1900552.
10 S. Topp, V. Prasad, G. C. Cianci, E. R. Weeks and J. P. Gallivan, *J. Am. Chem. Soc.*, 2006, **128**, 13994–13995.
11 K. R. Raghupathi, J. Guo, O. Munkhbat, P. Rangadurai and S. Thayumanavan, *Acc. Chem. Res.*, 2014, **47**, 2200–2211.
12 C. Gu, A.-B. Jia, Y.-M. Zhang and S. X.-A. Zhang, *Chem. Rev.*, 2022, **122**, 14679–14721.
13 S.-L. Li, M. Han, Y. Zhang, G.-P. Li, M. Li, G. He and X.-M. Zhang, *J. Am. Chem. Soc.*, 2019, **141**, 12663–12672.
14 P. Murto and H. Bronstein, *J. Mater. Chem. C*, 2022, **10**, 7368–7403.
15 Z.-M. Chen, X.-M. Zhang and Y.-Q. Tu, *Chem. Soc. Rev.*, 2015, **44**, 5220–5245.
16 L. Ji, J. Shi, J. Wei, T. Yu and W. Huang, *Adv. Mater.*, 2020, **32**, 1908015.
17 I. J. Al-Busaidi, A. Haque, N. K. Al Rasbi and M. S. Khan, *Synth. Met.*, 2019, **257**, 116189.
18 J. Yang, X. Zhen, B. Wang, X. Gao, Z. Ren, J. Wang, Y. Xie, J. Li, Q. Peng, K. Pu and Z. Li, *Nat. Commun.*, 2018, **9**, 2963–2973.
19 B. Wu, Y. Liu, Y. Zhang, L. Fan, Q.-Y. Li, Z. Yu, X. Zhao, Y.-C. Zheng and X.-J. Wang, *J. Mater. Chem. A*, 2022, **10**, 12489–12496.
20 Y. Rout, A. Ekbote and R. Misra, *J. Mater. Chem. C*, 2021, **9**, 7508–7531.
21 X. Pan, C. Fang, M. Fantin, N. Malhotra, W. Y. So, L. A. Peteanu, A. A. Isse, A. Gennaro, P. Liu and K. Matyjaszewskit, *J. Am. Chem. Soc.*, 2016, **138**, 2411–2425.
22 Z. Xie, C. Chen, S. Xu, J. Li, Y. Zhang, S. Liu, J. Xu and Z. Chi, *Angew. Chem., Int. Ed.*, 2015, **54**, 7181–7184.
23 S. Revoju, A. Matuhina, L. Canil, H. Salonen, A. Hiltunen, A. Abate and P. Vivo, *J. Mater. Chem. C*, 2020, **8**, 15486–15506.
24 M. Zhai, Y. Miao, H. Wang, L. Wang, X. Ding, C. Chen and M. Cheng, *Dyes Pigm.*, 2022, **202**, 110279.
25 M. Okazaki, Y. Takeda, P. Data, P. Pander, H. Higginbotham, A. P. Monkman and S. Minakata, *Chem. Sci.*, 2017, **8**, 2677–2686.
26 J. K. Salunke, F. L. Wong, K. Feron, S. Manzhos, M. F. Lo, D. Shinde, A. Patil, C. S. Lee, V. A. L. Roy, P. Sonar and P. P. Wadgaonkar, *J. Mater. Chem. C*, 2016, **4**, 1009–1018.
27 K. M. Vengaian, C. D. Britto, K. Sekar, G. Sivaraman and S. Singaravadivel, *Sens. Actuators, B*, 2016, **235**, 232–240.
28 Y. Yoon, S. Shin and M. W. Shin, *ACS Appl. Mater. Interfaces*, 2022, **14**, 4220–4229.
29 M. Garcia-Iglesias, K. Peuntinger, A. Kahnt, J. Krausmann, P. Vazquez, D. Gonzalez-Rodriguez, D. M. Guldi and T. Torres, *J. Am. Chem. Soc.*, 2013, **135**, 19311–19318.
30 A. Jimenez-Almarza, A. Lopez-Magano, R. Mas-Balleste and J. Aleman, *ACS Appl. Mater. Interfaces*, 2022, **14**, 16258–16268.

31 S. Jagtap, M. K. Yenkie, N. Labhsetwar and S. Rayalus, *Chem. Rev.*, 2012, **112**, 2454–2466.
32 U. Manna, G. Das and M. A. Hossain, *Coord. Chem. Rev.*, 2022, **455**, 214357.
33 P. P. Hujoel, *Nutrients*, 2022, **14**, 4263–4295.
34 V. Amendola, G. Bergamaschi, M. Boiocchi, L. Fabbrizzi and M. Milani, *Chem. – Eur. J.*, 2010, **16**, 4368–4380.
35 Y. Zhou, J. F. Zhang and J. Yoon, *Chem. Rev.*, 2014, **114**, 5511–5571.
36 V. S. Padalkar and S. Seki, *Chem. Soc. Rev.*, 2016, **45**, 169–202.
37 W. Wu, M. Wang, J. M. Ma, Y. L. Cao and Y. H. Deng, *Adv. Electron. Mater.*, 2018, **4**, 1800185.
38 S. H. Yan, K. P. Abhilash, L. Y. Tang, M. Yang, Y. F. Ma, Q. Y. Xia, Q. B. Guo and H. Xia, *Small*, 2019, **15**, 1804371.
39 Y. Wang, X. Jia, E. B. Berda, J. Zhao, X. Liu and D. Chao, *Eur. Polym. J.*, 2020, **138**, 109979.
40 D. P. Dubal, N. R. Chodankar, D.-H. Kim and P. Gomez-Romero, *Chem. Soc. Rev.*, 2018, **47**, 2065–2129.
41 H. Sun, S. Liu, W. Lin, K. Y. Zhang, W. Lv, X. Huang, F. Huo, H. Yang, G. Jenkins, Q. Zhao and W. Huang, *Nat. Commun.*, 2014, **5**, 3601–3610.
42 V. K. Thakur, G. Ding, J. Ma, P. S. Lee and X. Lu, *Adv. Mater.*, 2012, **24**, 4071–4096.
43 L. Striepe and T. Baumgartner, *Chem. – Eur. J.*, 2017, **23**, 16924–16940.
44 G. He, G. Li, L. Xu, W. Zhang, K. Zhou, Y. Ding, F. Liu and X. He, *Angew. Chem., Int. Ed.*, 2018, **57**, 4897–4901.
45 X.-Q. Zhu, Z. Dai, A. Yu, S. Wu and J.-P. Cheng, *J. Phys. Chem. B*, 2008, **112**, 11694–11707.
46 A. F. Buene and D. M. Almenningen, *J. Mater. Chem. C*, 2021, **9**, 11974–11994.
47 Z. Liu, E. Shi, Y. Wan, N. Li, D. Chen, Q. Xu, H. Li, J. Lu, K. Zhang and L. Wang, *J. Mater. Chem. C*, 2015, **3**, 2033–2039.
48 S. M. Sartor, C. H. Chrisman, R. M. Pearson, G. M. Miyake and N. H. Damrauer, *J. Phys. Chem. A*, 2020, **124**, 817–823.
49 Z. Li, Q. Dong, Y. Li, B. Xu, M. Deng, J. Pei, J. Zhang, F. Chen, S. Wen, Y. Gao and W. Tian, *J. Mater. Chem.*, 2011, **21**, 2159–2168.
50 W. P. Lustig, S. Mukherjee, N. D. Rudd, A. V. Desai, J. Li and S. K. Ghosh, *Chem. Soc. Rev.*, 2017, **46**, 3242–3285.
51 L. Ji, S. Griesbeck and T. B. Marder, *Chem. Sci.*, 2017, **8**, 846–863.
52 W.-D. Zhang, G. Li, L. Xu, Y. Zhuo, W.-M. Wan, N. Yan and G. He, *Chem. Sci.*, 2018, **9**, 4444–4450.
53 S. Zhang, X. Yang, X. Liu, L. Xu, B. Rao, N. Yan and G. He, *J. Mater. Chem. C*, 2021, **9**, 4053–4061.
54 M. Boiocchi, L. Del Boca, D. E. Gomez, L. Fabbrizzi, M. Licchelli and E. Monzani, *J. Am. Chem. Soc.*, 2004, **126**, 16507–16514.
55 C. Bhaumik, S. Das, D. Maity and S. Baitalik, *Dalton Trans.*, 2011, **40**, 11795–11808.
56 T. Kundu, A. D. Chowdhury, D. De, S. M. Mobin, V. G. Puranik, A. Datta and G. K. Lahiri, *Dalton Trans.*, 2012, **41**, 4484–4496.
57 X. Sun, Y. Qi, H. Liu, J. Peng, K. Liu and Y. Fang, *ACS Appl. Mater. Interfaces*, 2014, **6**, 20016–20024.
58 N. Yan, W. Zhang, G. Li, S. Zhang, X. Yang, K. Zhou, D. Pei, Z. Zhao and G. He, *Mater. Chem. Front.*, 2021, **5**, 4128–4137.
59 R. Song, G. Li, Y. Zhang, B. Rao, S. Xiong and G. He, *Chem. Eng. J.*, 2021, **422**, 130057.
60 S. Zhang, L. Ma, W. Ma, L. Chen, K. Gao, S. Yu, M. Zhang, L. Zhang and G. He, *Angew. Chem., Int. Ed.*, 2022, **61**, e202209054.
61 S. Zhuang, X. Li and J. Liu, *Dyes Pigm.*, 2021, **193**, 109464.
62 A. F. Buene, N. Uggerud, S. P. Economopoulos, O. R. Gautun and B. H. Hoff, *Dyes Pigm.*, 2018, **151**, 263–271.

